

Interaction of antiprotons with Rb atoms and a comparison of antiproton stopping powers of the atoms H, Li, Na, K, and Rb

Armin Lühr · Nicolas Fischer · Alejandro Saenz

Received: date / Accepted: date

Abstract Ionization and excitation cross sections as well as electron-energy spectra and stopping powers of the alkali metal atoms Li, Na, K, and Rb colliding with antiprotons were calculated using a time-dependent channel-coupling approach. An impact-energy range from 0.25 to 4000 keV was considered. The target atoms are treated as effective one-electron systems using a model potential. The results are compared with calculated cross sections for antiproton-hydrogen atom collisions.

Keywords antiproton · collision · alkali-metal atom · stopping power · energy spectrum · ionization · excitation

PACS 34.50.Bw · 34.50.Fa

1 Introduction

The motivation for studying antiproton (\bar{p}) collisions is manifold and only a selection of motives shall be mentioned here. First of all, there is a general interest in collisions with exotic particles. Second, \bar{p} scattering is a fundamental collision system due to the fact that the projectile is heavy and has a negative charge resulting in several advantages. For example, antiprotons do not capture electrons leading essentially to a one-center problem. They approximately follow a classical path down to velocities slower than the Bohr velocity. And even very slow \bar{p} are still able to ionize making the investigation of “adiabatic” collisions possible. Third, a comparison of results obtained from \bar{p} and p scattering yields differential information on the collision process.

The present motivation originates also from other aspects. One is the facility design for the Facility for Antiproton and Ion Research (FAIR) including the Facility for Low-energy Antiproton and Ion Research (FLAIR). In order to set the requirements of the (low-energy) \bar{p} storage rings correctly the influence of residual-gas atoms and molecules on the \bar{p} beam has to be known. Therefore, quantities like the stopping power or the

Institut für Physik, AG Moderne Optik, Humboldt-Universität zu Berlin, Hausvogteiplatz 5-7, D-10117 Berlin, Germany.
 Tel.: +49-(0)30-2093-4814
 E-mail: Armin.Luehr@physik.hu-berlin.de

diffraction of the \bar{p} beam due to collisions are of interest. Furthermore, a theoretical data base of \bar{p} cross sections for various atomic and molecular targets should be provided in view of future experiments at the Antiproton Decelerator (AD) at CERN and also under improved conditions at the upcoming FLAIR.

During the last decades advances have been achieved in the understanding of \bar{p} collisions with the simplest one- and two-electron atoms H and He. However, in the case of $\bar{p} + \text{He}$ experiment and theory did not agree for impact velocities below the mean electron velocity of the ground state for more than a decade stimulating a vivid theoretical activity. The discrepancy has been partly resolved by very recent measurements on $\bar{p} + \text{He}$ by Knudsen *et al.* [3].

On the other hand, the literature on \bar{p} collisions with alkali-metal atoms is sparse. No measurement has been performed so far and only two calculations for Li and Na targets by Stary *et al.* [10] as well as by McCartney and Crothers [8], and recently results for Li, Na and K atoms [4] were presented. This is in contrast to the fact, that alkali-metal atoms are in principal theoretically and experimentally feasible due to their electronic shell structure. All core electrons fill inner closed shells while a single valence electron occupies an outer s ($l = 0$) state.

In this work results for ionization and excitation in \bar{p} collisions with Rb atoms are discussed and compared to previous findings for the alkali-metal atoms Li, Na and K [4] as well as to calculations with an atomic H target. Electron-energy spectra are determined and are exemplarily shown for Rb. Furthermore, electronic stopping powers are presented for \bar{p} collisions with Li, Na, K and Rb. The used method has already been discussed elsewhere in some detail [4]. Therefore, only the major approximations, the description of the target atoms, as well as the general concept are briefly reviewed in the following section. Atomic units are used unless otherwise stated.

2 Method

The collision process is considered in a semi-classical way using the impact parameter method. Thereby, the electrons of the target atoms are treated quantum mechanically while the projectile moves on a straight classical trajectory $\mathbf{R}(t) = \mathbf{b} + \mathbf{v}t$ given by the impact parameter \mathbf{b} and the velocity \mathbf{v} which are parallel to the x and z axis, respectively and t is the time.

An effective one-electron description $\Psi(r, t)$ of the collision process is used

$$i \frac{\partial}{\partial t} \Psi(\mathbf{r}, t) = \left(\hat{H}_0 + \frac{-Z_p}{|\mathbf{r} - \mathbf{R}(t)|} + \frac{Z_p}{|\mathbf{R}(t)|} \right) \Psi(\mathbf{r}, t), \quad (1)$$

where \mathbf{r} is the electron coordinate, Z_p is the charge of the projectile, and \hat{H}_0 is the time-independent target Hamiltonian. Ψ is expanded in eigenstates ϕ_j of $\hat{H}_0 = -\frac{1}{2} \nabla^2 + \hat{V}_{\text{mod}}(r)$ centered on the target nucleus. The model potential V_{mod} used for the effective one-electron description of the alkali-metal atoms was proposed by Klapisch [2] and the potential parameters are taken from [9]. The radial part of the ϕ_j is expanded in B-spline functions while the angular part is expressed in spherical harmonics.

The expansion $\Psi = \sum_j c_j(t) \phi_j$ leads to coupled differential equations for the expansion coefficients $c_j(t)$ for every trajectory, i.e., for every b and impact energy $E = M_p \mathbf{v}^2 / 2$ with M_p being the antiproton mass. The cross section σ_j for an explicit

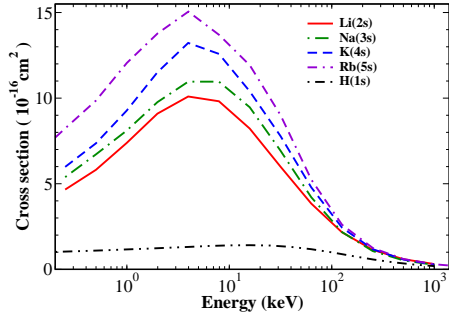


Fig. 1 Ionization cross section σ_{ion} for $\bar{p} + \text{Rb}$ collisions compared with Li, Na, K, and H [4] targets as function of the impact energy E . Solid curve, Li; dash-dotted curve, Na; dashed curve K; double-dash-dotted curve, Rb; dash-doubly-dotted curve, H.

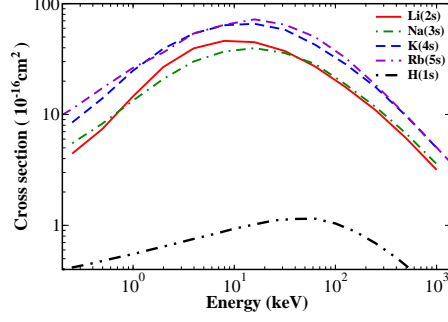


Fig. 2 Excitation cross section σ_{ex} for $\bar{p} + \text{Rb}$ collisions compared with Li, Na, K, and H [4] targets as function of the impact energy E . Solid curve, Li; dash-dotted curve, Na; dashed curve K; double-dash-dotted curve, Rb; dash-doubly-dotted curve, H.

E for a transition from the initial state to ϕ_j is given by

$$\sigma_j = 2\pi \int |c_j(t \rightarrow \infty, b)|^2 b db, \quad (2)$$

where the cylindrical symmetry of the collision system has been used. The electronic energy loss cross section is then given by

$$S = \sum_j (\epsilon_j - \epsilon_1) \sigma_j, \quad (3)$$

where ϵ_1 and ϵ_j are the energies of the ground and the j -th state, respectively. The cross sections for ionization and excitation are given by the sum of all σ_j in Eq. (2) for transitions into states ϕ_j with positive and negative energies ϵ_j , respectively.

3 Results

The method was extensively tested by studying its convergence behavior and, additionally, by detailed comparisons of proton (p) cross sections obtained with the same approach with literature results [4]. Also, a detailed comparison to the two already mentioned works [8,10] which address \bar{p} collisions with Li and Na can be found in [4]. Furthermore, the present method was successfully applied to the calculation of collisions including an H_2 target treated as an effective one-electron system [5,6]. Therefore, no further testing of the method is presented here.

3.1 Ionization

The ionization cross sections for \bar{p} collisions with Rb are compared in Fig. 1 to the results for Li, Na, K and H [4]. It can be seen that the curves for all alkali-metal atoms share the same qualitative behavior. They differ, however, in the magnitudes of the maxima which are order according to the chemical element. The larger the group

number in the periodic table the higher the maximum of the ionization cross section. While this ordering is also prominent at low energies the differences between the atoms vanish at high impact energies.

For comparison also the well known ionization cross sections for $\bar{p} + \text{H}$ collisions are given in Fig. 1. Similar results for H might be expected since it is in the same group in the periodic table as the alkali-metal atoms. However, there are also obvious differences. Namely, the magnitudes of the cross sections for the alkalis and the H atom differ considerably and only become comparable at high impact energies $E \geq 500$ keV. Also the position of the maximum for H is shifted from ≈ 5 keV for the alkalis to ≈ 25 keV for H. The differences of the magnitudes of the ionization curves among the alkalis as well as between the alkalis and the H atom in Fig. 1 can be explained with the different ionization potentials of the target atoms [4].

A comparison to the results for p collisions is not shown here. However, it should be mentioned that the findings for p differ considerably from those for \bar{p} for energies $E < 100$ keV [4]. For these energies the electron loss in the case of p impact is much larger than for \bar{p} collisions. This is due to the fact that electron capture becomes the dominant loss process at low p impact energies which is excluded for \bar{p} .

3.2 Excitation

In Fig. 2 the excitation cross sections for \bar{p} collisions with Rb are compared to the results for Li, Na, K and H [4]. Again, all curves for the alkali-metal atoms share the same qualitative behavior but differ in the magnitudes of their maxima. The maxima are, however, not ordered by chemical element. Here, Li lies above Na. The maxima of the curves are at higher impact energies — Na, K, Rb ≈ 15 keV and Li ≈ 8 keV — compared to ionization. In absolute values all curves lie clearly above the results for ionization in Fig. 1 whereas the curves for Li and Na as well as for K and Rb are close to each other. On the other hand, the slope of the curve for Li is more similar to that of K and that of Na more similar to that of Rb.

A comparison to the results for excitation of the H atom where the maximum is around 50 keV shows that the difference is even larger than in the case of ionization. The differences for excitation among the alkalis as well as between the alkalis and the H atom can be explained with the different excitation energies, especially for the lowest excited p state ($l = 1$) which is the most prominent transition at high and intermediate E [4]. The excitation energy for the $1s - 2p$ transition in H with 0.375 a.u. is in particular large compared to, e.g., the $5s - 5p$ with 0.058 a.u. for Rb.

A comparison of the \bar{p} excitation results to p collisions with alkalis yields, in contrast to ionization, no large differences [4]. This could have been expected since no additional excitation mechanism for one of the two projectiles exists. However, smaller differences for \bar{p} and p impact exist and will be discussed elsewhere.

3.3 Electron-energy spectra

Besides total cross sections for ionization and excitation also differential information can be extracted from the collision process. In Fig. 3 the electron-energy spectrum, i.e., the cross section that an electron is emitted with the energy ϵ is presented for a Rb atom target. The spectra of the other alkali-metal atoms Li, Na, and K were also

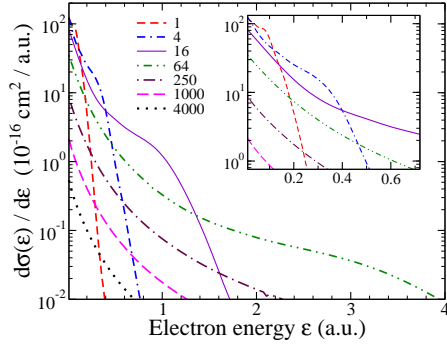


Fig. 3 Electron-energy spectra for $\bar{p} + \text{Rb}$ collisions as a function of the energy ϵ of the emitted electron. Spectra are shown for seven different \bar{p} impact energies (keV): 1, 4, 16, 64, 250, 1000, and 4000. The inset shows the region of small ϵ enlarged.

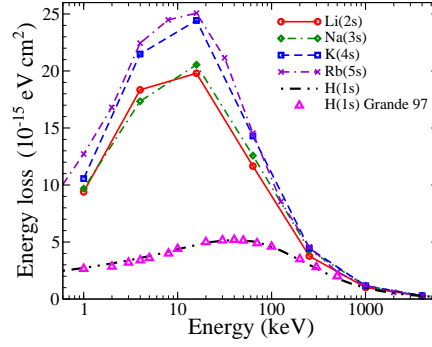


Fig. 4 Energy loss cross section for \bar{p} collisions with Li, Na, K, Rb and H as function of E . Solid curve, Li; dash-dotted curve, Na; dashed curve K; double-dash-dotted curve, Rb; dash-double-dotted curve, H; triangles, H, Grande and Schiwietz [1].

determined. They are qualitatively comparable to that of Rb and are therefore not shown here. Spectra for seven different \bar{p} impact energies $1 \leq E \leq 4000$ keV are given. All curves are smooth, fall off with increasing ϵ and no resonance structures can be seen for \bar{p} impact which is also the case for $\bar{p} + \text{H}_2$ collisions [5]. This is in contrast to the spectra for electron loss in the case of p collisions where a pronounced resonance can be observed for $\epsilon = E/M_p = \mathbf{v}^2/2$ [7]. The resonance originates from the electron capture process by the p . Thereby, the ionized and then captured electron moves with approximately the velocity \mathbf{v} of the p .

For lower impact energies E the maxima of the spectra at $\epsilon \rightarrow 0$ are higher and the decrease of the curve with increasing ϵ is steeper. For small electron energies $\epsilon \rightarrow 0$ the curves are ordered according to their impact energy E . For larger electron energies $\epsilon > 0$ the spectra all share the same behavior. Always the uppermost curve crosses all lower-lying curves belonging to larger E . This is nicely illustrated in the inset in Fig. 3; first for the spectrum for $E = 1$ keV and then for that for $E = 4$ keV. Consequently, the mean kinetic energy of the ionized electrons $\bar{\epsilon}$ increases for larger impact energies E of the \bar{p} .

3.4 Stopping power

The obtained differential information on ionization and excitation can be used for the determination of the cross section for electronic energy loss also referred to as stopping power $S(E)$. Results for \bar{p} collisions with Li, Na, K, Rb, and H are shown in Fig. 4. A comparison of the present findings for $\bar{p} + \text{H}$ with an atomic orbital calculation by Grande and Schiwietz [1] yields good agreement and confirms therefore the present implementation.

As could have been expected from the results for ionization and excitation the electronic energy loss for H targets is smaller than for the alkali-metal atoms. On the other hand, the difference of $S(E)$ between H and alkali-metal atoms is, especially for high E , not very large. This can be understood regarding Eq. (3) where the σ_j are weighted with the excitation energies ($\epsilon_j - \epsilon_1$) which are clearly larger for excitations

of an H atom. The differences for Li and Na observed for ionization and excitation compensate each other for the electronic energy loss. Also, the results for K and Rb are very similar. In general, it is possible to conclude that in the case of \bar{p} impact the electronic stopping power of alkali-metal atoms is dominated by the excitation process. Therefore, a large stopping power can be found for all alkali-metal atoms at $E \approx 15$ keV in a narrow impact energy range when considering the energy loss on a linear E scale.

4 Outlook

Besides the electron-energy spectrum also the angular distribution of the ionized electrons can be analyzed in order to obtain doubly-differential cross sections since the wave function Ψ is fully known (at every time step). Currently, the method is extended to treat also molecular targets. Calculations for H₂ using a one-electron model potential of the target have already been performed [5,6]. A further development including a full two-electron description of the collision process is in progress which considers also molecular properties. Once a two-electron description is implemented it can be used for atomic targets, too. In the limit of vanishing internuclear distance, e.g., He atoms could be used in order to test the implementation. But also calculations for, e.g., alkaline earth metals can easily be done, if again model potentials are used.

Acknowledgements The authors are grateful to BMBF (FLAIR Horizon) and *Stifterverband für die deutsche Wissenschaft* for financial support.

References

1. Grande, P.L., Schiwietz, G.: Coupled-channel calculations of the electronic energy loss. Nucl. Instrum. Methods Phys. Res. B **132**, 264 (1997)
2. Klapisch, M.: A program for atomic wavefunction computations by the parametric potential method. Comput. Phys. Commun. **2**, 239 (1971)
3. Knudsen, H., Kristiansen, H.P., Thomsen, H., Uggerhøj, U. *et al.*: Ionization of helium and argon by very slow antiproton impact. Phys. Rev. Lett. **101**, 043201 (2008)
4. Lühr, A., Saenz, A.: Antiproton and proton collisions with the alkali-metal atoms Li, Na, and K. Phys. Rev. A **77**, 052713 (2008)
5. Lühr, A., Saenz, A.: Antiproton collisions with molecular hydrogen. Phys. Rev. A **78**, 032708 (2008)
6. Lühr, A., Vanne, Y.V., Saenz, A.: Parameter-free one-center model potential for an effective one-electron description of molecular hydrogen. Phys. Rev. A **78**, 042510 (2008)
7. Lühr, A., Saenz, A.: Collisions of low-energy antiprotons with molecular hydrogen: ionization, excitation and stopping power. Hyperfine Interact. (2008)
8. M. McCartney and D. S. F. Crothers: The single ionization of multielectron atoms using the continuum-distorted-wave eikonal-initial-state model. J. Phys. B **26**, 4561 (1993)
9. Magnier, S., Aubert-Frécon, M., Hanssen, J., Sech, C.L.: Two-electron wavefunctions for the ground state of alkali negative ions. J. Phys. B **32**, 5639 (1999)
10. Stary, C., Lüdde, H.J., Dreizler, R.M.: Optical potential description of collisions of p and \bar{p} with alkali atoms. J. Phys. B **23**, 263 (1990)